Design and Development of an Efficient Multilevel DC/AC Traction Inverter for Railway Transportation Electrification

Mohamed Z. Youssef, *Senior Member, IEEE*, Konrad Woronowicz, *Senior Member, IEEE*, Kunwar Aditya, *Member, IEEE*, Najath Abdul Azeez, *Student Member, IEEE*, and Sheldon S. Williamson, *Senior Member, IEEE*

***Abstract*—This paper presents a new trend in the transportation industry to adopt the multilevel inverter-based propulsion systems and gives the design procedure of a new dc/ac three-phase six-level inverter for powering the rail metro cars. The proposed inverter is based on the multilevel converter as it possesses much lower component voltage stress compared with the pulsewidth-modulated (PWM) topologies. Space vector pulsewidth modulation (SVPWM) with back-to-back clamped diode voltage modulation operation is used to achieve voltage regulation and high efficiency at any loading condition. Zero-current-switching operation is achieved without using an auxiliary circuit, which leads to minimum switching losses. The novelty of the proposed inverter lies within the proposed control methodology, which uses a new switching pattern that guarantees a modified SVPWM to eliminate the unwanted harmonics from the output voltage. The new algorithm is developed using numerical iterative solution using the Newton–Raphson technique that was downloaded to the processor using digital signal processing developed code. The mathematical model is simple but proven to be effective. As a result, a higher operating efficiency at full load of 98.5% is achieved as compared to previous efficiency of 97%. Analytical, simulation, and experimental results of a 1500 Vdc/700 Vac 400-kW converter are presented to offer the proof of concept. The converter provides real estate savings for the train under floor layout, higher operating efficiency as well as better cost price than the conventional two-level PWM hard-switched converters.**

***Index Terms*—Electric vehicles, power electronics, traction motors, transportation, vehicles.**

I. Introduction

THE soaring fuel prices and the universal trend for green energy with a friendly environment zero carbon foot print have inspired the work toward less energy consumption in the transportation industry. In addition and recently, provincial and federal governments have initiated zero carbon foot print tax credit for transit agencies to deploy greener trains. Since less energy means less hydrobill and more tax rebates; this new trend has raised the competition bar for working efficiency of the inverters' used in the rail transit industry to above 98% from the traditional 92% achieved by the hard-switched two-level pulsewidth-modulated (PWM) inverters. Global developments in the semiconductor industry have resulted in the production of high power IGBTs that can operate at high switching frequencies up to 40 kHz; with reasonable economical price. Multilevel inverters have the advantage of operating at higher frequencies without any major electromagnetic interference (EMI) levels, unlike the traditional two-level PWM converters [1]; thanks to the lower dv/dt values of the output voltages. In addition, the high-frequency operation of the multilevel inverters allow a reduced real estate for the inverter in the under floor or the ceiling layout, which is a big advantage. This has allowed more space for other auxiliary powering devices, to accommodate the need for more onboard newly introduced devices such as security cameras, onboard internet access points, and advertisement panels. This reduced foot print of the propulsion inverter comes with a lesser weight because of higher switching frequency capabilities; hence, a reasonable reduction of the energy consumption of the vehicle is expected. Other transit agencies foresee this as a good chance to attain more revenue, as the weight reduction of the inverter can allow boarding more passengers. The PWM converters have a dramatically low working efficiency levels at high switching frequency, in addition to the need of additional auxiliary resonant circuitry during the switch transition period to achieve zero-current switching (ZCS) for the IGBT switches. As a result, in practice within the rail industry, these converters need to work at low switching frequencies and this will require them to have a large space envelope for the same power level compared with the multilevel inverters. In order to get an optimal foot print for the traction inverter, the switching frequency must be increased. Based on the fact that multilevel converters can operate at higher frequencies, thanks to the recent developments of the IGBTs, industry's interest is growing toward these converters, especially with the price drop of the IGBT semiconductors. Nowadays, multilevel inverters are also superior to the resonant inverters because of the cost, efficiency, and the associated reduction in EMI. By the time the EMI filters are added to the resonant inverters; they end up with a larger foot print than that of the multilevel inverters [2]–[10]. Multilevel inverters with coupled inductor were proposed in [7], but this solution is very difficult to adjust when implementing for the real

Manuscript received November 10, 2014; revised April 21, 2015 and February 10, 2015; accepted June 1, 2015. Date of publication June 22, 2015; date of current version November 30, 2015. Recommended for publication by Associate Editor D. Vinnikov.

M. Youssef, K. Aditya, N. A. Azeez, and S. S. Williamson are with the, Department of Electrical, Computer and Software Engineering, University of Ontario Institute of Technology, Oshawa ON L1H 7K4, Canada (e-mail: mohamed.youssef@uoit.ca, kunwar.aditya@uoit.ca, najath.azeez@uoit.ca, Sheldon.williamson@uoit.ca).

K. Woronowicz is with the Bombardier, Kingston K7K 2H6, Canada (e-mail: konrad.woronowicz.2013@ieee.org).

Color versions of one or more of the figures in this paper are available online at http://ieeexplore.ieee.org.

Digital Object Identifier 10.1109/TPEL.2015.2448353

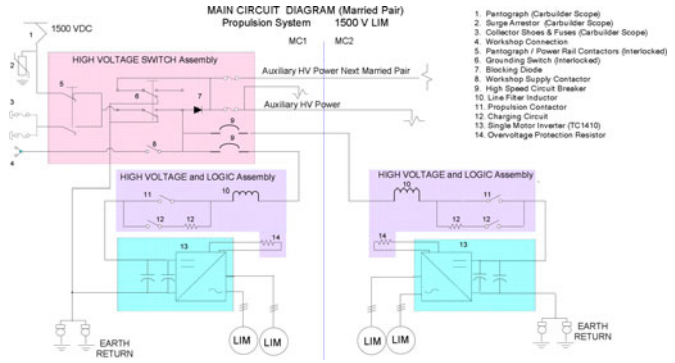

Fig. 1. Overall schematics of the powering system with two inverters powering two LIMs.

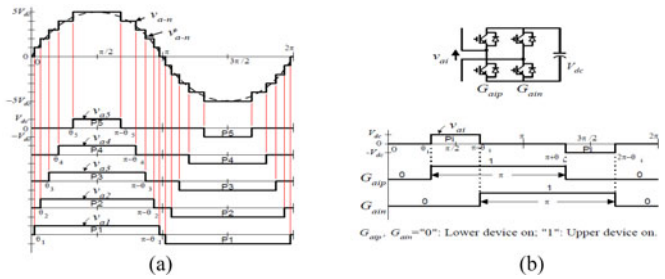

Fig. 2. Generic switching pattern of the proposed selective harmonic elimination technique.

power levels of the train; as it is very expensive and inefficient. In [11], new switching patterns were introduced to reduce the total harmonic distortion (THD) of the current by 25–30%, but it affects the design effort for the converters. It is also questionable at very high frequencies and high power levels as transient conditions may result in very brief short-circuit periods. In [12]–[15], novel switching techniques to reduce the harmonic content of the output voltage of the inverter were presented, with limitations on the implementation of the controller for the actual rail high power levels. In [16], new PWM switching patterns were presented and developed to minimize the THD, but with a lot of hardware complications and high mathematical efforts. In [17] discontinuous and continuous and continuous PWM techniques has been compared for three-level neutral-point-clamped voltage source Inverter widely used in high power, medium voltage application. In this paper, a six-level converter (see Fig. 1) is proposed and analyzed with a new switching pattern that guarantees the elimination of the unwanted harmonics from the output voltage waveform. The inverter's output voltage is controlled by variable SVPWM technique, provided that it is always clamped to a maximum level so as not to affect the insulation of the linear induction motor (LIM) or the voltage stress on the semiconductor IGBT switches, in a sequence made to guarantee the ZCS operation of the IGBTs. The outer control loop helps regulating the output voltage. The presented converter is shown in Fig. 1, illustrating the power path from the wayside rail to the LIM through the inverter and protection circuitry.

The small footprint of the proposed multilevel inverter is a good fit for some applications where powering from either an overhead catenary system or a wayside rail is desired (like the transit system in Guangzhou, China). The isolation circuit is designed for a smooth transition between the overhead catenary and the wayside rail. Simulation model was built in PSIM with the parameters calculated through Transit Studio software as explained in the following section and results will be reported after the design section. The proposed idea is very simple to implement without the need to do very rigorous mathematical work as in [1]. A very systematic approach was presented in [2] to minimize the harmonics but with a trial and error process for the modulation index, which is tricky.

II. Back-to-Back Diode-Clamped Converter Drive and the Selective Harmonic Elimination

The selective harmonic elimination stepped waveform (see Fig. 2) will minimize the THD content of the output voltage of the inverter [1]

$$\mathrm{v}(t) = \sum_{1,3}^{\infty} \frac{4v_{\mathrm{dc}}}{n\pi} \begin{pmatrix} \cos(n\theta_1) \\ \cos(n\theta_2) \\ +\cos(n\theta_3) + \\ \cdots + \cos(n\theta_s) \end{pmatrix} \cos(n\omega t). \quad (1)$$

In order to cancel the harmonics of the output voltage, the summation of these harmonics should be equal to zero. A sequence of the switching angles shall be chosen to achieve the following equation:

$$\cos(n\theta_1) + \cos(n\theta_2) + \cdots + \cos(n\theta_s) = 0. \quad (2)$$

In the aforementioned equation, assuming a polynomial to solve the problem using the resultant theory will result in a new set of equations, as follows.

For the fundamental frequency

$$P_1(x_1, x_2, x_3) = \sum_{1}^{3} x_n - m = 0. \quad (3)$$

For the third harmonic

$$P_1(x_1, x_2, x_3) = \sum_{1}^{3} 4x_n^3 - 3x_n = 0. \quad (4)$$

For the fifth harmonic

$$P_1(x_1, x_2, x_3) = \sum_{1}^{3} 5x_n - 20x_n^3 + 20x_n^5 = 0. \quad (5)$$

Here, $P_1(X_1, X_2, X_3)$ is polynomial with X_1, X_2, X_3 as variables. X_1, X_2, X_3 represents θ_1, θ_2, and θ_3, respectively. X_n is used to represents θ_n.

As a first step, the Newton–Raphson method is used to solve the aforementioned equations using an initial guess, and then, forming the Jacobians. One can find that the solution will be in the following form:

$$(x_1, x_2, x_3) = (\theta_1, \theta_2, \theta_3) = (8.7^\circ, 28.7^\circ, 54.9^\circ). \quad (6)$$

These values were obtained for the cancellation of the odd harmonics of the inverter output voltage. The asymmetry of the

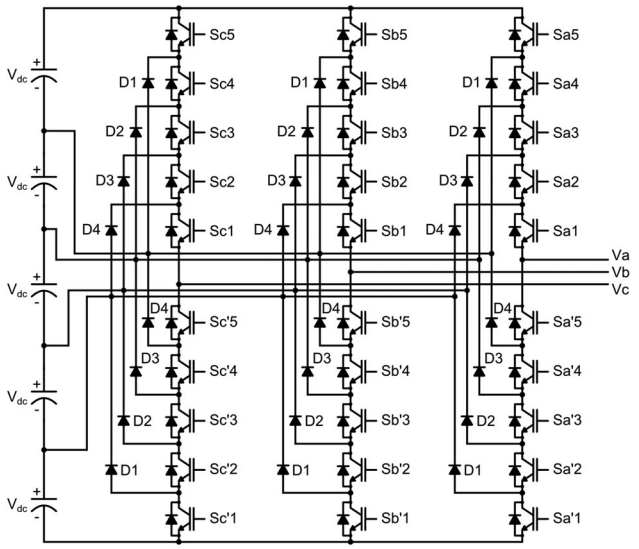

Fig. 3. Circuit schematics of the proposed inverter.

Output V_a	Switch State									
	S_{a5}	S_{a4}	S_{a3}	S_{a2}	S_{a1}	$S_{a'5}$	$S_{a'4}$	$S_{a'3}$	$S_{a'2}$	$S_{a'1}$
$V_5 = 5V_{dc}$	1	1	1	1	1	0	0	0	0	0
$V_4 = 4V_{dc}$	0	1	1	1	1	1	0	0	0	0
$V_3 = 3V_{dc}$	0	0	1	1	1	1	1	0	0	0
$V_2 = 2V_{dc}$	0	0	0	1	1	1	1	1	0	0
$V_1 = V_{dc}$	0	0	0	0	1	1	1	1	1	0
$V_0 = 0$	0	0	0	0	0	1	1	1	1	1

Fig. 4. Switching states of the different switches of the converter.

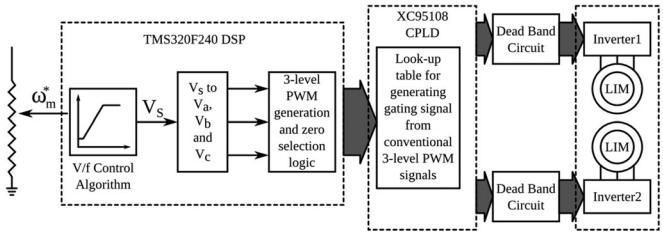

Fig. 5. Drive scheme of the dual inverter vehicle propulsion system.

phase angles will determine the maximum value of the switching frequency as the leading edge time of the IGBT is fixed. This is to avoid short circuiting two legs of the inverter. The controller algorithm for the converter is programmed using C++ and the digital signal processing (DSP) card from an iZotope Company, Boston, MA, USA, is loaded with the code. Thanks to the harmonic cancellation, there is no need for a dv/dt filter between the inverter and motor, which saves weight and size of the inverter. Fig. 3 shows the schematic of the proposed six-level cascaded inverter with clamped diodes to control the maximum voltage stress of all the switches. The switching sequence is given in Fig. 4, with the firing angles calculated to control the amount of harmonics generated in the output voltage of the inverter. Fig. 5 shows the block diagram of the controller. Here, the required

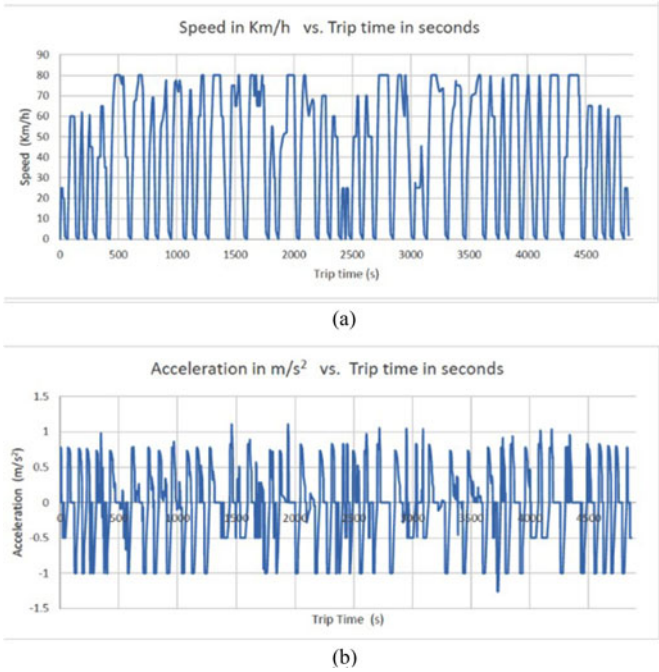

Fig. 6. (a) Speed profile along the GZL6 alignment. (b) Acceleration profile along the GZL6 alignment.

six-level switching signals are generated from the conventional three-level PWM.

III. Input Design Requirements

In order to size the converter, the root mean square input current has to be calculated as follows.

1) The alignment of the route has to be defined; as a case study we used the Guangzhou alignment in China.
2) The speed profile and the acceleration profile have to be defined. Fig. 6 shows the speed and acceleration profile for the alignment.
3) The input data about the vehicle weight and dimensions have to be entered.
4) The data from 1 to 3; have to be entered in "Transit Studio" software; to calculate the current profile of each motor needed to pull the train weight as per the speed and acceleration profile.
5) From the calculated current, power factor, motor efficiency, and voltage profile of the motor, the loading conditions are determined for the inverter design.

Fig. 7 shows the instantaneous motor current for a round trip out and in to the depot. Using this curve, the RMS current for each motor is 249.26 A. This is the design requirement for sizing the inverter IGBT driver circuit and the input filter circuit.

The calculated energy consumption for each car with auxiliaries is calculated to be 255.3 kW·h/car. This number is calculated under the worst case scenario, when the line is 100% receptive. The input choke of the inverter shall be designed to carry this amount of the inductor and the energy requirement will require that value of the inductor. Hence, the input inductor was sized to be of 2.2 mH, with a current

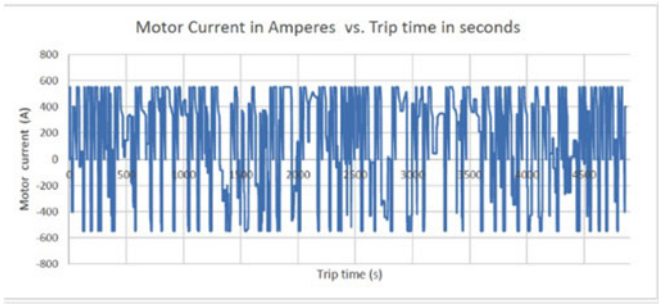

Fig. 7. Instantaneous values of the input motor current along the round trip.

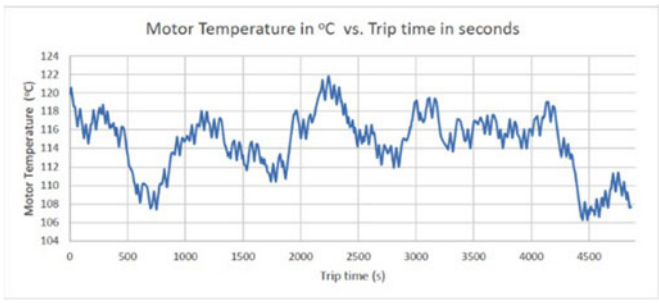

Fig. 8. Instantaneous values of the Motor Temperature.

TABLE I
TEST PARAMETERS FOR PROPOSED POWER SUPPLY

Parameter	Value
V_{in}	1500 V±20%
V_{outmax}	1300 Vac±5%
IGBT switches	*6s*FF1000R17IE4* (3 300 V)
I_{o}	350 A (Full-load)
Diode Blocking Voltage	3000, 6000, 9000, 12000 V
Snubber Capacitors	6.8 nF
LIM	136-kW rated power at 0.65 maximum power factor and 0.73 maximum efficiency

carrying capacity of 260 A rms. This is to satisfy the round trip time of 43.26 min of the train car. Fig. 8 shows the instantaneous motor temperature for a round trip. This temperature curve along with the amperage loading value was used to select the type of the IGBT of the inverter as per Table I. The complete input filter design procedure is given in [18]. Fig.9 gives the instantaneous efficiency of motor at each instant of a round trip.

IV. SIMULATION EXPERIMENTAL RESULTS

Simulation of the proposed converter is performed using PSIM software in order to validate the design procedure given in the preceding sections. Table I shows the converter parameters used in the layout.

A. ZCS

Fig. 10 shows the waveforms of the phase current and voltage of one phase through the IGBT Bridge at high loading conditions. The current always lags the inverter output voltage

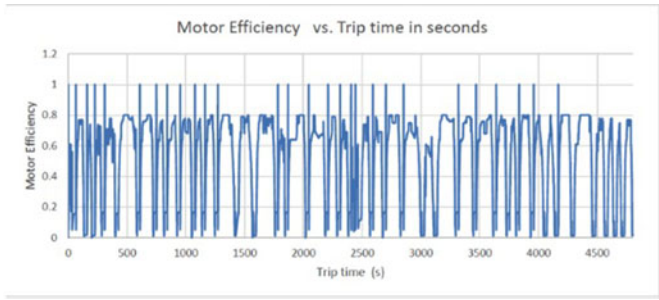

Fig. 9. Motor efficiency instantaneous values.

and crosses zero inside of the nonzero voltage pulse at output of the inverter, resulting in the required current to reset the snubber capacitors and provide ZCS. The IGBT current and voltage are synchronized with almost sinusoidal waveforms and was measured using an ac current clamp transducer with a factor of 1:30 A, attached to the IGBT phase in the inverter box on the train.

The Fourier frequency transform (FFT) of the output inverter voltage shows that the maximum THD has value of 6.4%. According to EU standards inrush current should be maximum three times the full-load current. As shown in Fig 11, inrush current is only 110% of full-load current, and therefore, is well below the standard norms.

B. Efficiency and EMI

Table II gives the efficiency of the proposed inverter versus the loading condition at a nominal input voltage of 1500 Vdc. In addition, the efficiency was measured at low input voltage of 900 Vdc and full-loading conditions, which is the worst operating condition, as the third rail voltage may drop down by 20%. The recorded efficiency was about 87.5%, which is good for an emergency situation that can rarely happen in the lifetime of the car. It is worth to mention that the values of the efficiency surpass the hard-switched converters in the industry by at least 5% [12]–[13]. The inverter was tested on the bench given in Appendix and results reported in Table II.

Fig. 12 shows the photo of the inverter prototype. Serial communication port of the prototype and its top view has been shown in fig. 14 and 15 respectively for more clarity on the hardware layout. Fig. 13 shows the FFT of output voltage of the inverter. Depending on the type of the rail system, there are different standards for radiated emission. For 750-V DC rail, EMI limit has been shown with blue line. Fig. 13 distinctively shows the EMI limits for the different rail system by color coding. Blue line shows the maximum limit of radiated EMI for 750V DC rail as per standards. The FFT of output voltage was far below all the standards limit.

V. CONCLUSION

A new family of the transportation converters is proposed in this paper. A new switching pattern was introduced to eliminate the predefined harmonic content of the inverter output voltages. These harmonics are determined based on the type of the rail system and the inverter topology. The numerical solution

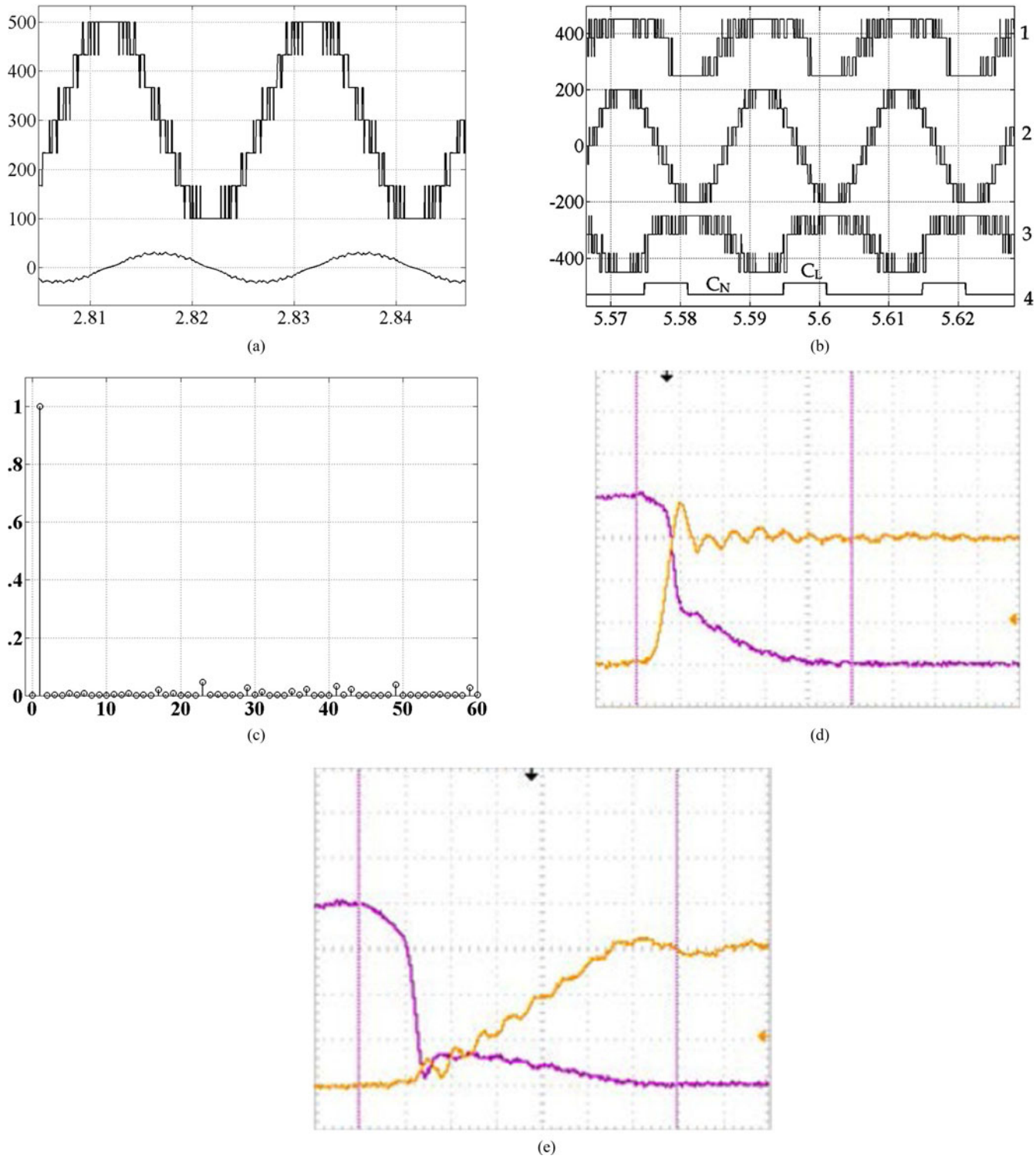

Fig. 10. Experimental results: Voltage, current, FFT at full load (a) Phase voltage and current. (b) Phase voltages of the inverter. (c) FFT of the phase voltage. (d) IGBT current and voltage without snubber. (e) IGBT current and voltage with snubber.

allows for the development of a specific switching pattern for every alignment, which guarantees the elimination of the harmonics. The new family has a minimal EMI level with reduced common-mode voltage. The code is developed and downloaded to the converter processor using the DSP code. In addition, they enjoy a very high operating efficiency, which might save an energy bill of $1M worth for the life time of the vehicles. Simulation results prove the achievement of the required wayside and customer specifications. Finally, the experimental results show that the proposed converter can achieve ZCS,

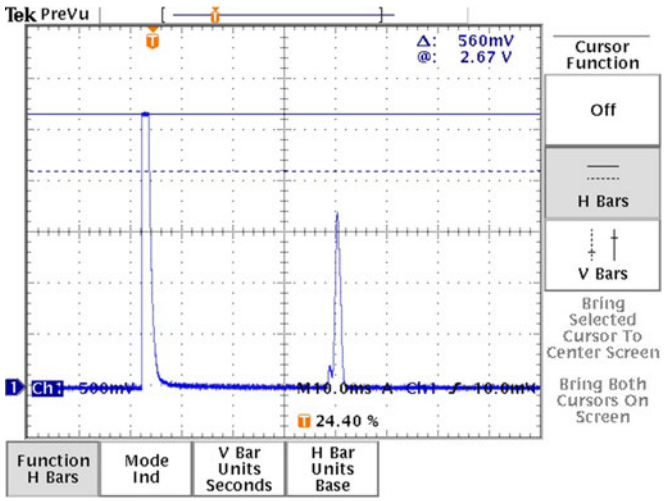

Fig. 11. Experimental Results: Inrush starting current is less than 110% of the full-load current as per the EN50155 standards: Sound design of input filter

TABLE II
OVERALL EFFICIENCY VERSUS LOADING CONDITIONS

Load (%)	V_{in} (DC input voltage)	I_{in} (RMS DC input current)	Efficiency (η%)
5%	1500 V	50 A	94.9
25%	1500 V	100 A	96.5
50%	1500 V	150 A	97.1
75%	1500 V	200 A	98.2
100%	1500 V	250 A	99

higher working efficiencies. The photos in the appendix show the smaller footprint of the converter box. A case study of GZL6 alignment in China was used to design the inverter. The cost of development is $40 000 USD, which is cheaper than the typical current price of $60 000 USD.

APPENDIX
PICTURES OF THE DEVELOPED INVERTER

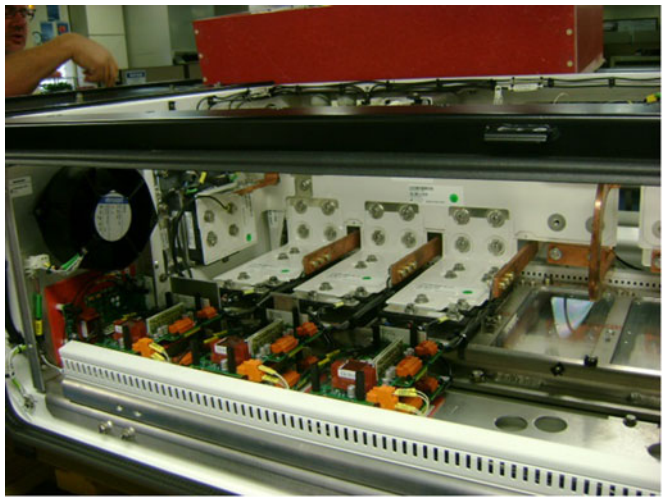

Fig. 12. Inverter prototype.

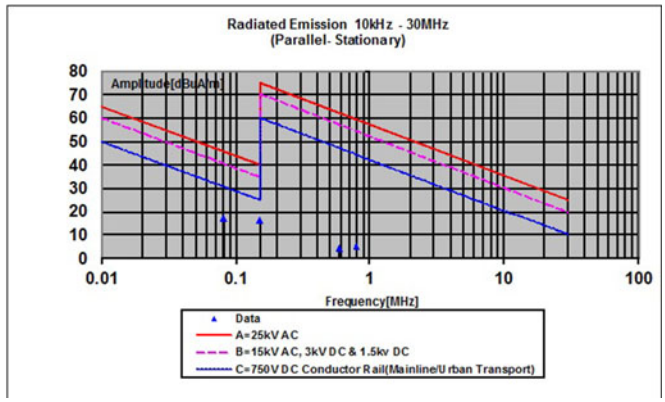

Fig. 13. EMI test data well below the standard limits.

Fig. 14. Photo of the developed prototype for the traction converter (serial ports of communication systems).

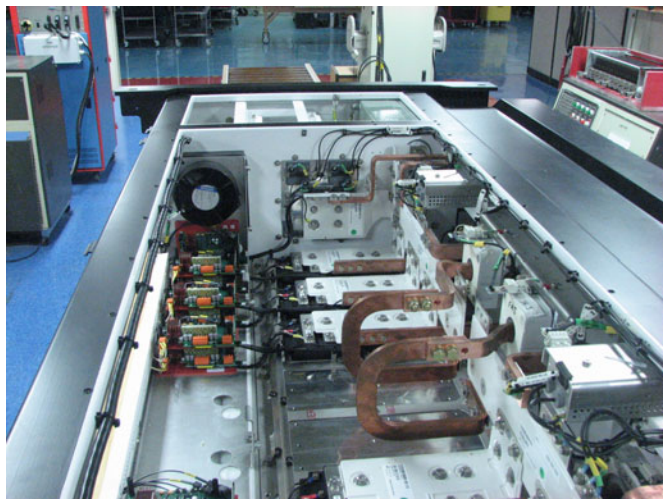

Fig. 15. Top view of the inverter layout.

REFERENCES

[1] S. Maritheus, "Systematic design of high performance hybrid cascaded multi inverters with active voltage balance and minimum switching losses," *IEEE Trans. on Power Electron.*, vol. 28, no. 7, pp. 3100–3113, Jul. 2013.

[2] D. Ahmadi, K. Zou, and F. Wang, "A universal selective harmonic elimination method for high power inverters," *IEEE Trans. Power Electron.*, vol. 26, no. 10, pp. 2743–2752, Oct. 2011.
[3] T. Kejellqvist, S. Ostlund, and S. Norrga, "Active snubbber circuit for source commutated converters utilizing the IGBTin the linear region," *IEEE Trans. Power Electron.*, vol. 23, no. 5, pp. 2595–2601, Sep. 2008.
[4] K. Fuji, P. Kollensperger, and R. W. Doncker, "Characterization and comparison of high blocking voltage IGBTs and IEGTs under hard and soft switched conditions," *IEEE Trans. Power Electron.*, vol. 23, no. 1, pp. 172–179, Jan. 2008.
[5] E. S. Kim and Y. H. Kim, "A ZVZCS PWM FB DC/DC converter using a modified energy recovery snubber," *IEEE Trans. on Industrial Electronics.*, vol. 49, pp. 1120–1127, Oct. 2002.
[6] J. Dudrik, P. Spanik, and N. D. Trip, "Zero voltage and zero current switching full-bridge dc-dc converter with auxiliary transformer," *IEEE Trans. Power Electron.*, vol. 21, no. 5, pp. 1328–1335, Sep. 2006.
[7] A. Knight, J. Salmon, and J. Ewanchuk, "Single phase multilevel PWM Inverters using Coupled Inductors," *IEEE Trans. Power Electron.*, Vol. 24, no. 5. pp. 1259–126, Mar. 2009.
[8] J. E. Slotine and W. Li, *Applied Nonlinear Control*, 1st ed. Englewood Cliffs, NJ, USA: Prentice Hall, 1991.
[9] J. Z. Tsypkin, *Relay Control Systems*, 1st ed. Cambridge, U.K.: Cambridge Univ. Press, 1984.
[10] Y. Xiaomin and I. Barbi, "Fundamentals of a new diode clamping diode multilevel inverter," *IEEE Trans. Power Electron.*, vol. 15, no. 4, pp. 711–718, Jul. 2000.
[11] S. Das and G. Narayannan, "Novel switching sequences for multilevel inverters," *IEEE Trans. Ind. Electron.*, vol. 59, no. 3, pp. 1477–1487, Feb. 2012.
[12] G. Gopinath, A. S. A. Mohamed, and M. R. Baiju, "Fractal based space vector PWM for multilevel inverters-A novel approach," *IEEE Trans. Ind. Electron.*, vol. 56, no. 4, pp. 1230–1237, Apr. 2009.
[13] W. J. Lee, C. E. Kim, G. W. Moon, and S. K. Han, "A new phase-shifted full-bridge converter with voltage-doubler type rectifier for high-efficiency PDP sustaining power module," *IEEE Trans. Ind. Electron.*, vol. 55, no. 3, pp. 2450–2458, Jul. 2008.
[14] R. Dolecek, O. Carney, V. Lonek, and V. Schejbal, "Disturbing effects in rail vehicle traction drive," in *Proc. Int. Conf. Electronika*, 2012, pp. 1–4.
[15] X. Chen, D. Liang, and W. Zhang, "Braking traction recovery with supercapacitor and bidirectional DC-DC converters," in *Proc. IEEE Power Electron. Motion Control Conf.*, Harbin, China, 2012, pp. 879–883.
[16] G. Narayanan, D. Zhaao, K. Krishnamurthy, and A. Ayyannar, "Space Vector based PWM techniques for reduced current ripple in multilevel inverters," *IEEE Trans. Ind. Electron.*, vol. 55, no. 4, pp. 1614–1627, Apr. 2008.
[17] T. Bruckner and D. G.Holmes, "Optimal pulse width modulation for three level inverters," *IEEE Trans. Ind. Electron.*, vol. 20, no. 1, pp. 82–89, Jan. 2005.
[18] M. Youssef, M. Orabi, and J. AbouQahouq, "The electromagnetic design considerations for an input filter of a 3-phase inverter for the transportation industry," in *Proc. IEEE Energy Convers. Conf. Expo.*, 2010. 4210–4216.

Mohamed Z. Youssef (SM'08) received the Ph.D. degree in power electronics from PEARL Lab, Queen's University, Kingston, Canada in 2005.

He was also an adjunct Assistant Professor involved in teaching and research at Queen's University. In 2007, he joined Bombardier Transportation, where he worked as a Senior Research and Development Engineer. In 2012, he joined Alstom Transport as a Research and Development Engineering Manager. His research interests include electromechanical systems for the transportation industry, electromagnetic compatibility for the railways and power electronics applications for the information technology. He was the Motor and Electronics Manager for Armstrong Pumps before coming back to Academia.

He is an Assistant Professor in the Department of Electrical, Computer, and Software Engineering Department, University of Ontario Institute of Technology (UOIT), Oshawa, Canada. He is also the Director of Power Electronics and Drives Lab, UOIT. He has more than 60 papers in the top tier IEEE journals and conferences with five US/Canadian patents. He is a Professional Engineer in the province of Ontario, Canada.

Konrad Woronowicz (M'13–SM'13) received the B. Sc. and M. Sc. degrees from the Technical University of Szczecin, Szczecin, Poland and the Ph. D. degree from the West Pomeranian University of Technology, Szczecin.

Since 1995, he has been with Bombardier Transportation, Kingston, Canada, working on various transportation systems and R&D projects and played a key role in the development of LIM-based mass transit systems for New York, Beijing, Vancouver, and Kuala Lumpur among others. He is currently a Fellow Expert and his current interests include electromagnetic design for wireless power transfer for electric traction and automotive applications, high-performance linear motors, special permanent magnet motors, and energy storage.

Kunwar Aditya (M'14) received the B.E. degree in electrical engineering with distinction from Bharati Vidyapeeth University, Pune, India, in 2009, and the M.Tech. degree (Hons.) in electrical engineering from the Indian Institute of Technology (Banaras Hindu University), Varanasi, India, in 2012. He is currently working toward the Ph.D. degree in electrical engineering from the University of Ontario Institute of Technology, Oshawa, Canada.

His research Interest includes electric vehicles, inductive charging and control of power electronics converters.

Najath Abdul Azeez (S'04) received the B.Tech. degree from the National Institute of Technology, Calicut, India, in 2003 and the M.Tech. and Ph.D. degrees from the Indian Institute of Science, Bangalore, India, in 2008 and 2014, respectively.

He is currently working as a Postdoctoral fellow at the University of Ontario Institute Of Technology, Oshawa, Canada. His research interests include the areas of power converters and drives.

Sheldon S. Williamson (S'01–M'06–SM'13) received the B.E. degree in electrical engineering with high distinction from the University of Mumbai, Mumbai, India, in 1999, and the M.S. and Ph.D. degrees (Hons.) in electrical engineering from the Illinois Institute of Technology, Chicago, IL, USA, in 2002 and 2006, respectively.

From June 2006 to June 2014, he held a tenure-track Assistant Professor position, followed by a tenured Associate Professor position, in the Department of Electrical and Computer Engineering, Concordia University, Montreal, Canada. He is currently an Associate Professor in the Department of Electrical, Computer, and Software Engineering, University of Ontario Institute of Technology, Oshawa, Canada. His research interests include transportation electrification, electric energy storage systems, and automotive power electronics/motor drives.